The Planetary Science Journal, 2:150 (14pp), 2021 August https://doi.org/10.3847/PSJ/ac1272

Exploration of Icy Ocean Worlds Using Geophysical Approaches

Angela G Marusiak[1], Steven Vance[1], Mark P Panning[1], Marie Běhounková[2], Paul K Byrne[3,4], Gaël Choblet[5], Mohit Melwani Daswani[1], Kynan Hughson[6], Baptiste Journaux[7], Ana H Lobo[8], Britney E Schmidt[6], Kateřina Pleiner Sládková[2], Krista M Soderlund[9], WenZhan Song[10], Ondřej Souček[11], Gregor Steinbrügge[12], Andrew F. Thompson[8], and Sili Wang[10]

[1] Jet Propulsion Laboratory, California Institute of Technology, 4800 Oak Grove Drive, Pasadena, CA 91109, USA; angela.g.marusiak@jpl.nasa.gov, angela.marusiak@gmail.com
[2] Charles University, Faculty of Mathematics and Physics, Department of Geophysics, V Holešovičkách 2 18000 Praha 8, Czech Republic
[3] Department of Marine, Earth, and Atmospheric Sciences, North Carolina State University, Raleigh NC 27695, USA
[4] Department of Earth and Planetary Sciences, Washington University in St. Louis, St. Louis, MO 63130, USA
[5] Université de Nantes, Laboratoire de Planétologie et Géodynamique, UMR 6112, 2 rue de la Houssiniére, Nantes F-44322, France
[6] School of Earth and Atmospheric Sciences, Georgia Institute of Technology, 311 Ferst Drive, Atlanta, GA 30332, USA
[7] University of Washington, Department of Earth and Space Sciences, Seattle, WA 98915, USA
[8] California Institute of Technology, 1200 E. California Boulevard, Pasadena, CA 91125, USA
[9] Institute for Geophysics, Jackson School of Geosciences, The University of Texas at Austin, J.J. Pickle Research Campus, Bldg. 196, 10100 Burnet Road (R2200), Austin, TX 78758, USA
[10] University of Georgia, 200 D.W. Brooks Drive, Athens, GA 30602, USA
[11] Charles University, Sokolovská 83, 186 75 Praha 8, Czech Republic
[12] Department of Geophysics, Stanford University, 397 Panama Mall, Stanford, CA 94305, USA
Received 2021 February 9; revised 2021 May 20; accepted 2021 June 28; published 2021 August 5

Abstract

Geophysics-focused missions and improved geophysical data sets are critical for the future exploration of icy ocean worlds. Of particular interest is the exploration of the Galilean moon, Europa, and the Saturnian moons, Titan and Enceladus. These bodies likely have geologically active surfaces and may harbor habitable subsurface environments. Placing any candidate signatures for life in context requires further knowledge of the interior of these worlds. While the surfaces of these bodies have been mapped, their interiors remain poorly understood. Geophysical approaches such as geodesy, seismology, ice-penetrating radar and altimetry measurements, and electromagnetometry would provide critical information regarding the interior of these icy ocean worlds. The approaches described below would answer key science questions regarding ice shell and ocean dynamics, internal structure and interior layer thicknesses, near-surface structure, and how material from the deep interior might be exchanged with the surface. Here we outline the geophysical environments of Enceladus, Europa, and Titan; some outstanding science questions that remain to be addressed; and examples of the geophysical approaches that can provide the context to better understand icy ocean worlds.

Unified Astronomy Thesaurus concepts: Geodesics (645); Magnetohydrodynamics (1964); Lunar seismology (973); Galilean satellites (627); Saturnian satellites (1427); Ocean planets (1151)

1. Introduction

Icy ocean worlds are of substantial interest to the planetary community for several reasons, including the potential habitability of their subsurface oceans and their geologically active surfaces. We focus on the bodies of Europa, Titan, and Enceladus due to the unique science opportunities each moon would present. Previous missions, namely the Galileo (Carr et al. 1998; Greeley et al. 1998) and Cassini–Huygens missions (Elachi et al. 2005; Porco et al. 2006; Iess et al. 2014), were able to image most of these moons' surfaces and provide some constraints on their internal structure (Figure 1). However, many science questions still remain. Specifically, the internal structure and dynamics of the ice shells and oceans are poorly understood. Geophysical approaches can offer a comprehensive view into the interiors of planetary bodies, including icy satellites. Additional science questions regarding the astrobiological potential of these worlds can be addressed by using a geophysical instrument suite. Data provided through geophysical observations are key to fully understand the context of sampled materials and to properly interpret the habitability and any putative signatures of life. Here we describe a suite of geophysical approaches that could provide these data.

Previous missions to icy ocean worlds returned data that suggest relatively young surfaces covering subsurface oceans (Kargel & Pozio 1996; Carr et al. 1998; Porco et al. 2006; Schenk & Zahnle 2007; Kirchoff & Schenk 2009). The ice shells of these bodies range from a few kilometers to tens of kilometers thick, making direct sampling of the subsurface oceans difficult, except for Enceladus (and possibly Europa), where active plumes deposit ocean material onto the surface. Surface observations of features such as plume activity (Porco et al. 2006; Sparks et al. 2016), tectonic features (Hoppa 1999; Greeley et al. 2000), observed albedos (Noll et al. 1995; Fagents et al. 2000), and lack of craters (Zahnle et al. 2003) indicate these bodies are likely geologically active today. Geophysical data sets such as seismic, gravity, ice-penetrating radar, topographic, and magnetic measurements can determine the current level of activity in the near surface and probe deeper into the interior.

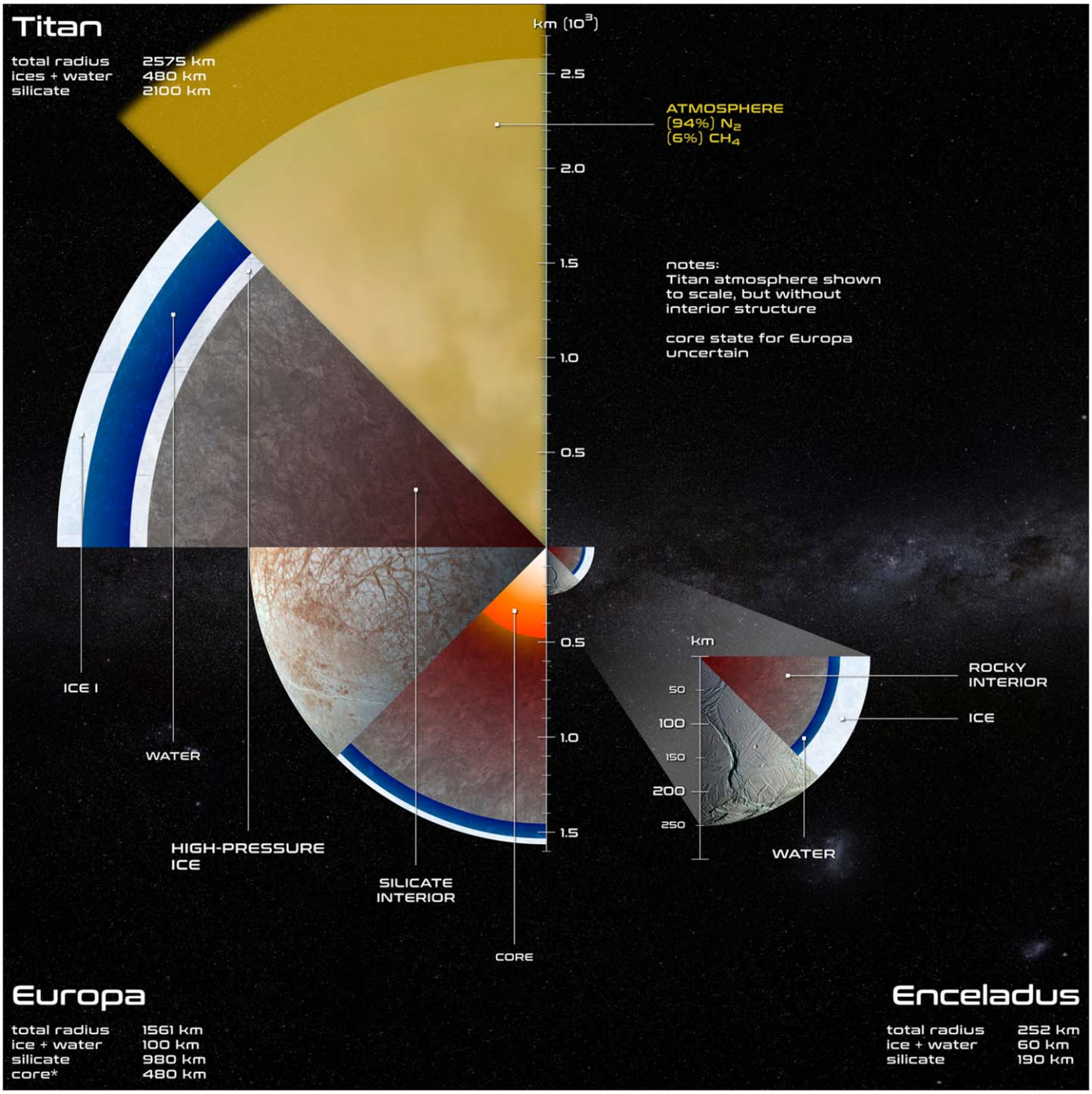

Figure 1. Schematic cross sections of three icy satellites we discuss: Titan, Europa, and Enceladus. All cross sections are to scale, but the depths to each component layer are only approximate (based on the interior structure models of Vance et al. 2018). Depths are given to the nearest 10 km, such that aggregate depths may not match known planetary radii values.

Geophysical measurements are vital for understanding the current thermal and physical state of the ice shells and for providing constraints on their internal evolution and current dynamics. The interior properties of these moons are the ultimate arbiters of the amount of energy available to sustain life. Light (solar energy) can be essentially ruled out as a source of energy for life in ice-covered ocean worlds. Hence, we focus on establishing the requirements of chemoautotrophic organisms (Schulze-Makuch & Irwin 2002). Life as we know it would be killed in short order by a lack of redox-sensitive species (chemical species that are able to exchange electrons), which amounts to removing the source of energy for life. However, thermal energy can be supplied to the ocean by the decay of radioactive elements in the rocky interiors and oceans and can be supplied to the interior of the moons through tidal heating. Heating in the rocky interior may lead to magmatism at the rock–ocean interface (Waite et al. 2017; Běhounková et al. 2021). Tidal dissipation can occur in solid layers as well as the subsurface oceans (Moore & Hussmann 2009; Matsuyama et al. 2018; Čadek et al. 2019; Rovira-Navarro et al. 2019; Souček et al. 2019; Běhounková et al. 2021). For small icy worlds, rocky interiors can remain fragmented with

interstitial ice/liquid water. This is expected to soften the silicate core of the moon and lead to a strong increase in tidal deformation (see Roberts 2015 addressing the example of Enceladus). In the case of a core filled with liquid water, tidal heat can expedite water–rock interactions (Choblet et al. 2017), which can alter the ocean's composition through changes in element flux and alter the rocky core through carbonation (Glein & Waite 2020). For Europa and Enceladus, water–rock interactions might provide the chemical energy and materials for life while also controlling the ocean's chemistry including ionic strength and pH (Russell et al. 2014, 2017; Barge & White 2017). Geophysical models have helped predict Earth's seawater composition over history (Halevy & Bachan 2017). Likewise, determining the modern composition of the moons' oceans and fluids can therefore help reconstruct the global thermal and tidal evolutions. On Titan, rock–ocean interactions and exchange of material might be restricted by the presence of high-pressure ices beneath the subsurface ocean (Journaux et al. 2020b).

Oceanographic processes also play an important role in habitability. Thermal convection within the ocean may be driven by heating at the ocean bottom and cooling at the ice–ocean interface (Vance & Goodman 2009; Soderlund et al. 2014; Soderlund 2019; Amit et al. 2020). In addition to radioactive decay, mechanical drivers such as libration and tidal forcing may also contribute to ocean circulation and provide additional sources of heat within the oceans (Soderlund et al. 2020 and references therein). At Europa, electromagnetic pumping may similarly drive ocean flows (Gissinger & Petitdemange 2019). Variations in ice melting and freezing could sustain the observed pole-to-equator ice thickness gradients of Enceladus and Titan (Kvorka et al. 2018; Čadek et al. 2019), which would influence ocean flows (Zhu et al. 2017) and potentially support a global overturning circulation that connects low and high latitudes (Lobo et al. 2021). Melting and freezing of ice will introduce freshwater and brine to the subsurface ocean (Buffo et al. 2020; Vance et al. 2021b), further impacting large-scale heat and aqueous species transport (Jansen 2016; Kang et al. 2021; Lobo et al. 2021).

Heat and chemical transport may be expressed through tectonics. Although Earth is the only confirmed planetary body to currently exhibit plate tectonics, there are surface features of icy ocean worlds (e.g., strike-slip faults, extensional bands) that mirror some of the indicators of plate tectonics (Katterhorn & Hurford 2009; Kattenhorn & Prockter 2014; Bland & McKinnon 2017). Gravity, electromagnetic, radar, libration, deformation, and seismic measurements would be able to better measure the current rate of surface deformation, the average ice shell thickness, and the depth to the ice–ocean interface. Seismic and radar measurements, in particular, would help place estimates on the depth of the brittle–ductile transition and the thicknesses of the conductive and convective (if convection occurs) layers. A better understanding of the tectonic properties of icy satellites can determine the extent to which the interiors are coupled to the surfaces of these types of ocean worlds, providing better constraints for understanding the timescales of resurfacing and ice–ocean interactions and might even have implications for sustained habitability of the subsurface ocean.

Geophysical instrumentation can provide the data required to better understand internal layer interfaces and the dynamics within ice shells and any subsurface oceans. With improved estimates of ice shell thickness (and spatial variations), composition, and dynamics, the ice–ocean and ocean–rock interfaces can be better characterized and assessments of potential habitability improved. Seismology paired with gravity, electromagnetic (e.g., magnetotelluric), and radar studies can assess the depths of compositional and phase interfaces and infer the thermal state of the hydrosphere and possibly the deeper silicate interior. These studies can also characterize the current state of dynamics within the ice shell and fluid motions beneath the ice to infer how heat, redox-sensitive species, and components from the ocean might be transported between internal layers. Imaging and altimetry can provide topography and displacement measurements, which, paired with subsurface investigations, can better establish the current tectonic regime than image data alone. A geophysical sensor network deployed as part of a landed mission could sense and process multiple geophysical signals to compute a subsurface image in situ and in real time.

1.1. Enceladus

Enceladus may provide the lowest-cost mission to directly detect signatures of life. Materials from its oceans are readily accessible due to its active plumes, eliminating the need to drill through a thick ice shell (Postberg et al. 2011; Kite & Rubin 2016). Unlike the harsh radiation environment of Europa, the surface of Enceladus is not exposed to high levels of radiation that are likely to alter the chemical makeup of recently deposited material. Like Europa, Enceladus also experiences strong tidal forces from interactions with its primary. A region of particular interest on Enceladus is the so-called South Pole Terrain (SPT), a heavily tectonized region with its most prominent features being a set of fractures known as the "tiger stripes." In this region the ice shell may only be a few kilometers thick, as opposed to elsewhere where the ice shell may be tens of kilometers thick (Iess et al. 2014; McKinnon 2015; Beuthe et al. 2016; Čadek et al. 2016, 2019; Lucchetti et al. 2017; Hemingway & Mittal 2019; Rhoden et al. 2020).

Both orbiters and landers can carry payloads capable of geophysically exploring Enceladus (Ermakov et al. 2021; Mackenzie et al. 2021). An orbiter could provide improved topographic, structural, and thermal mapping (see Section 3.1) that would advance our understanding of the heat distribution and active features in the ice, the satellite's tectonic and geologic evolution, and how the plumes are sustained (Kite & Rubin 2016). Both vertical and lateral electrical conductivity profiles from electromagnetic (EM) sounding (see Section 3.2), ice-penetrating radar sounding (see Section 3.3), and geodetic data sets (see Section 3.4) would provide additional context to inform how ocean materials are transported through the ice shell. A lander that carries a seismometer (see Section 3.5) could determine the timing and location of seismicity around the SPT. Combining multiple in situ geophysical data sets would allow for real-time monitoring and detection of active faults and fractures (see Section 3.6). Enceladus is predicted to be less seismically active than Titan or Europa (Hurford et al. 2020), with only $\sim 10^{13}$ Nm being released per $\sim$1.4 Earth-day tidal cycle. However, because Enceladus is significantly smaller than Europa or Titan, any seismic event should be observable over a greater epicentral distance. Enceladus's relatively thin ice shell further increases the observed amplitudes of seismic phases compared to the thicker ice layers of Europa and Titan.

1.2. Europa

Europa's ice shell is likely 5–30 km thick, overlying an ocean that is about 100 km thick (Turtle & Pierazzo 2001; Nimmo et al. 2003; Nimmo & Schenk 2006; Travis et al. 2012; Howell 2020; Casajus et al. 2021). Due to the current uncertainty in plume activity, direct sampling of the ocean may be more elusive than on Enceladus. However, geophysical measurements, such as EM sounding, radar sounding, or seismology, might detect subsurface liquid pockets of water hypothesized to exist, for example, beneath chaos terrain (Schmidt et al. 2011) or as cryomagma chambers (Steinbrügge et al. 2020). These near-surface liquids may be easier to directly sample than the ocean, yet could contain ocean-derived material. Detection of such features would also provide context for understanding the thermal state and dynamics of the ice shell.

Europa's surface is covered in fractures and faults, suggesting a highly active surface. Europa's anticipated seismicity is higher than that of Earth (Panning et al. 2018; Hurford et al. 2020) and the greatest of the three bodies we focus on here. The main sources of Europa's seismicity are diurnal tides and forces from nonsynchronous rotation (McEwen 1986; Greenberg et al. 1998; Hoppa 1999; Greenberg et al. 2003; Hurford & Greenberg 2005; Wahr et al. 2006; Hurford et al. 2007; Sotin et al. 2009). Estimates suggest Europa will release $\sim 10^{16}$ Nm of seismic moment each ~3.5 Earth-day tidal cycle. This seismic energy amounts to roughly two orders of magnitude greater than that of the Moon over its ~27.3 Earth-day tidal cycle. A lander-based seismometer paired with an orbital altimeter would be able to detect surface displacements and determine the current rate of seismic activity. Deep events within Europa's ice shell could provide evidence of subsumption (Kattenhorn & Prockter 2014; Bland & McKinnon 2017), a process that is currently debated as a means of recycling portions of the ice shell akin to subduction on Earth (Johnson et al. 2017; Howell & Pappalardo 2019). Improved measurements of topography from orbit would also provide better parameters for modeling the dynamics and physical properties of Europa's near surface and help determine Europa's current tectonic regime. Maps of ice shell thickness could further be used to infer the distribution of heat flow from the ocean to the ice shell and estimate ocean circulations, as has been done for Enceladus (Čadek et al. 2019) and Titan (Kvorka et al. 2018).

1.3. Titan

Titan will experience seismicity from tidal cycles as well. Titan is anticipated to release $\sim 10^{15}$ Nm per ~15.9 Earth-day cycle. Unlike Europa and Enceladus, Titan has a thick, methane-rich atmosphere, and its cold surface (~90 K) allows for liquids such as methane and ethane to form stable lakes there. Both the atmosphere and these lakes will contribute to Titan's seismic background noise in a similar way to Earth's background signals from its oceans and atmosphere (Gutenberg 1947; Dybing et al. 2019). Storms with wind speeds above $2\ \mathrm{m\ s^{-1}}$ (Lorenz et al. 2012; Hayes et al. 2013) can produce globally or regionally observed signals, depending on the instrumentation (Stähler et al. 2019). Geophysical investigations of this moon would reveal its internal structure and, in particular, whether a layer of high-pressure ice exists between the ocean and silicate interior.

Geophysical instruments might also be able to detect the presence, or even estimate the abundances of, clathrates deep within Titan's ice shell by recovering the seismic velocity profile and returning estimates of the thickness of the conductive ice lid (Marusiak et al. 2020a). Clathrates can influence Titan's methane cycle and the thermodynamics of the ice shell (Lunine 2010; Mousis et al. 2015). Compared to pure-water ice, methane clathrates have a higher density, viscosity, and specific heat but a much lower thermal conductivity (Lunine & Stevenson 1985; Helgerud et al. 2003, 2009), which will influence the density, thermal structure, and dynamics of the ice shell (Kamata et al. 2019; Kalousová & Sotin 2020; Čadek et al. 2021). Determining if and where clathrates exist within Titan's ice shell will have implications for clathrates' role in Titan's methane cycle, the thermal evolution of the ice shell and ocean, and indirectly, Titan's habitability.

2. Evaluating Science Goals and Mission Architectures

Future missions to icy ocean worlds would address key science goals regarding large-scale internal state and structure, near-surface properties of the icy shell, as well as astrobiological potential. Although direct sampling of the subsurface oceans would be vital for detecting and understanding biosignatures, geophysical investigations can provide new context on the environment from which the samples came. Without knowledge of the chemical reactions and their energetics, mineral composition, and extent of water–rock interaction within these bodies, it would be difficult to discern the origin of potential biosignatures (Neveu et al. 2016). Below we outline contextual questions that could be addressed by geophysical measurements to assess internal environments and potential habitability.

To address these questions, both landers and orbiters are considered.

3. Methodologies and Approaches

Geophysical investigations can be carried out from both lander and orbiter platforms. Long-term observations would be limited by spacecraft fuel, lander power source, and/or environmental effects. For Enceladus, depending on inclination, an orbit would become unstable within tens of days without spacecraft corrections (Ermakov et al. 2021), so a landed geophysical mission could provide the opportunity to make observations over a longer time period. A landed mission would be limited by its power source supply. For Europa, the harsh radiation environment (Paranicas et al. 2007) would limit the mission lifetime of an orbiter and lander to only a few weeks, although instruments may be stored in a vault on the lander deck to decrease the effects of radiation and increase the lifetime of a lander (Hand et al. 2017). Missions to Titan are more amenable to long-term observations and would be limited by power supply rather than the environment. Below we discuss in more detail the approaches and instruments that appear in Table 1.

3.1. Imaging and Altimetry

High-resolution topographic data from stereo imaging by optical cameras, Light Detection And Ranging (LiDAR) instruments, or radars can greatly improve the geologic understanding of the key features of icy satellites (Kimura et al. 2019). On a regional scale, such data can facilitate the

Table 1
Science Development Guide for Geophysical Exploration of Ocean Worlds

Science Question	Science Objective	Science Measurements	Instrument
What are the physical state and layering properties that govern the structure and motion of the hydro-/cryosphere?	Determine thicknesses of ice shells and ocean	Reflections off ice–ocean and/or ocean–rock layers	Seismometer, radar sounder
		In situ inversion of multiple geophysical waves	Sensor network forming a subsurface camera
		Measure induction response	Magnetometer, magnetotellurics
		Measure libration and obliquity over several tidal cycles	Stereo imager, InSAR, optical imager, laser altimeter
		Determine regional and local topography	Laser altimeter, radar altimeter
		Measure h_2	Optical imager, laser altimeter, radar altimeter
		Measure k_2, Measure degree-2 gravity field	Gravity/radio science
	Determine if/where lateral heterogeneities occur	Measure density/gravity anomalies within the ice shell	Gravity ranger
		Search for variations in seismic arrival times and waveforms	Seismometer
		Search for variations in subsurface conductivity	Spacecraft magnetometer, (global scale), magnetotellurics, and transient electromagnetics (regional and local scale)
		Search for variations in radar reflection, absorption, and scattering	Radar sounder
Is the surface currently active, and how active if so?	Determine the current rate of seismicity	Detect, identify, and locate seismic events	Seismometer
	Determine the current rate of surface deformation	Measure surface displacements over several tidal cycles	Optical imager, InSAR, laser altimeter, radar altimeter
	Determine dynamics of near-surface in real-time	Continuous monitoring from in situ imaging from several geophysical measurements	Sensor network forming a subsurface camera
How, and at what rate, do ocean and ice shell processes transport heat and materials toward and away from the ice–ocean interface as well as toward the icy surface?	Determine if convection is occurring in the ice shell	Thermal profile via seismic profile	Seismometer
	Determine if the ocean is stratified or well-mixed	Measure density/gravity anomalies within the water column	Gravity ranger
		Characterize variations in radar reflection, absorption, and scattering	Radar sounder
		Characterize induction response of ocean column and circulation	Orbital or surface magnetometer, magnetotellurics
	Locate, determine the extent, and constrain the composition of brine and liquid pockets within the ice shell	Measure magnetic and conductivity anomalies in ice shell and resolve them vertically	Orbital magnetometer, surface magnetometer network, magnetotelluric network, transient electromagnetic network
		Search the ice shell for sharp reflectors with isostatically compensated ice thickness and surface elevation ratios; statistical analysis of near-surface return	Radar sounder and altimeter
		Continuous monitoring from in situ imaging from several geophysical measurements	Sensor network forming a subsurface camera
	Determine the resurfacing rates of the ice shell and seafloor. Investigate the main mechanisms behind resurfacing (e.g., volcanic burial, tectonic burial/reworking).	Create a high-resolution surface topography map	Stereo imager, laser altimeter, radar altimeter
		Determine current temporal rates of displacements and deformations	InSAR, stereo imager, optical imager, laser altimeter, radar altimeter

Table 1
(Continued)

Science Question	Science Objective	Science Measurements	Instrument
		Investigate tectonic setting based on located seismic responses	Seismometer
		Continuous monitoring from in situ computing and imaging from several geophysical measurements	Sensor network forming a subsurface camera
How is tidal dissipation distributed between the icy crust, ocean, and rocky core?	Determine the phase lag of tidal deformation	Measure imaginary part of h_2	Laser altimeter
		Measure imaginary part of k_2	Gravity ranger
	Determine the surface response to tidal forces	Measure radial surface displacements over several tidal cycles	Stereo imager, InSAR, optical imager, laser altimeter
How widespread are ongoing high-temperature water–rock interactions within these bodies and what is the rate of present-day hydrothermal activity?	Map the magnitude and spatial distribution of magnetization at the seafloor	Generate a global crustal magnetism map	Orbital magnetometer, magneto-telluric network
	Determine the magnitude and spatial distribution of gravity anomalies from seamounds, trenches, etc.	Gravity map of the seafloor	Gravity ranger
	Determine the magnitude and spatial distribution of seafloor minerals	Map of seafloor conductivity	Orbital magnetometer, magneto-telluric network
	Investigate seismicity associated with hydrothermal activity	Locate and characterize seismicity originating from the seafloor	Seismometer

understanding of tectonic and geologic features like the SPT on Enceladus and bands on Europa. On a global scale, laser altimetry can aid a gravity investigation and reveal long-wavelength topography, and on local scales enables detailed studies of local surface properties, including roughness. Stereo imaging and altimetry would also enable geodetic studies such as rotation state, including obliquity and librations (Steinbrügge et al. 2019), as well as radial tidal deformation (h_2) measurements (Steinbrügge et al. 2015). Combined with the measurement of the tidal Love number k_2, which can be inferred from gravity measurements, h_2 sets constraints on the ice shell thickness and rheology (Wahr et al. 2006). Interferometric Synthetic-Aperture Radar (InSAR) measurements completed over several orbits would allow for interferometric analysis to place constraints on diurnal horizontal and vertical ground motions. These measurements would help detect active fractures and can provide helpful constraints for determining ice shell thickness (Sandwell et al. 2004; Rignot et al. 2011). While altimetry is more sensitive to radial displacements, optical imaging would precisely determine the shell libration, an essential prerequisite for detecting subtle lateral displacements from faulting due to tidal deformation. For a lander-based system, measured changes in surface tilt would provide data for surface deformation. For Enceladus, the change in surface tilt is anticipated to vary by $\sim$4 μrad at the equator and reach tens of microrad regionally where the ice shell is thin or faults are present.

3.2. Electromagnetic Methods

Magnetic induction measurements from orbital and flyby-based magnetometers would complement seismic, radar, and gravity measurements by providing constraints on the conductivity and thickness of the subsurface ocean. This technique provided the most direct evidence for a present-day ocean in Jupiter's moon Europa (Kivelson et al. 2000), where observations from the Galileo mission's magnetometer detected a secondary magnetic field induced by periodic variations in the Jovian field associated with the nearly 10° tilt between the planet's magnetic pole and Europa's orbital plane. A magnetometer and plasma instrument suite will also feature prominently on NASA's upcoming Europa Clipper mission. In contrast, Saturn's magnetic field has no tilt with respect to its spin axis. However, it may be possible to investigate the properties of the Enceladus ocean using oscillations of the magnetic field due to orbital eccentricity. Also, active techniques like transient electromagnetics (TEM) may benefit from the relatively quiescent magnetic environment. Saturn's spin–magnetic axis alignment is also conducive to searching for magnetic induction signals generated by the flow of salty water within the satellite oceans, which might provide additional constraints on ocean dynamics (Vance et al. 2021c).

Lander-based passive and active approaches such as magnetotelluric (MT) and TEM methods, respectively, can detect fluid layers, reservoirs, and pathways within ice shells (Figure 2). As ion-laden liquids are more electrically conductive than solid ice, liquids can be detected and spatially resolved by their complex impedance signatures by measuring the frequency-dependent inductive currents. TEM utilizes transient pulses of current carried through loops placed on, or near, the surface to induce electric and magnetic fields in the subsurface. By quickly terminating these currents and measuring the decay response of the subsurface created by Lenz's law, a single TEM station can estimate the 1D vertical conductivity structure of the subsurface. Depending on the magnetic moment of the transmitter and the conductivity of the substrate, a single TEM sounding can have a depth of investigation of several tens of meters to a few kilometers and be able to resolve structures tens of meters thick (Grimm 2003). Alternatively, the passive MT method utilizes the natural variation of the electromagnetic environment around the target body of interest to infer subsurface electrical properties. Advantageously, MT

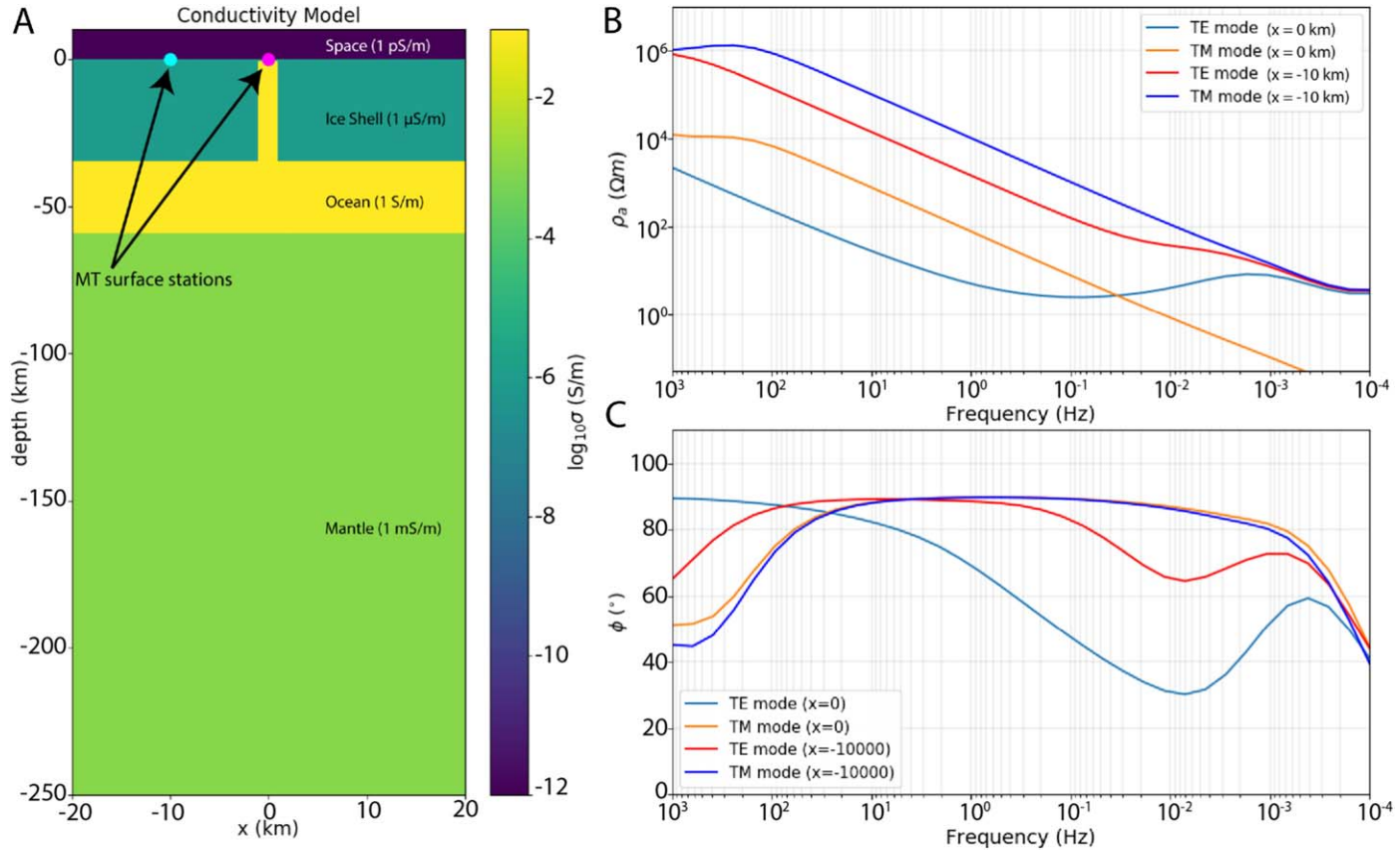

Figure 2. Example two-station MT survey near a conductive fluid-filled fracture zone (model extends both into and out of the page). The baseline between the two stations is 10 km while the fracture zone is 2 km wide and begins 500 m below the surface centered at $x = 0$ km. (A) The conductivity model (indicated by the color bar) includes a fracture through the ice shell (teal) filled from the ocean (yellow) above a silicate interior (light green). (B) The apparent resistivity (inverse conductivity) and (C) phase angle of the complex impedance as measured by the two MT stations. In this instance, the difference in the behavior of the transverse-electric (TE) and transverse-magnetic (TM) modes (the two independent polarization modes present in a 2D construction) at each station in the phase angle illustrates the departure from a uniformly layered subsurface, whereas the differences between the modes and stations in apparent resistivity help contextualize the magnitude and nature of this departure.

requires little a priori knowledge of the structure and natural variations of the target's electromagnetic environment (Grimm 2002). Taking advantage of time variations in the magnitude of the natural field, MT leverages the "skin-depth effect" by measuring the ratio of the orthogonal horizontal components of the surface electric and magnetic fields at a range of frequencies to reconstruct the vertical conductivity structure of the subsurface below the station (Grimm 2002). With sufficient frequency resolution, a broadband surface MT station measuring extremely low frequencies (approximately millihertz) to audio frequencies (approximately 10 kHz) would be able to resolve the 1D conductivity structure of the subsurface from a few meters below the surface to many kilometers with a vertical resolving power roughly equal to 0.5%–20% of the depth of penetration depending upon subsurface conductivity (Zonge & Hughes 1991). In both the case of TEM and MT, multiple 1D measurements from different geographical locations can be combined to create 2D or 3D electrical images of the subsurface with lateral resolution proportional to the station separations (Creighton et al. 2018).

While orbital and flyby-based magnetometers represent the most easily mobilizable EM investigation for interrogating the geophysical structure of ocean worlds, their spatial and depth resolution are limited by orbital mechanics, the conductive structure of the ocean world being observed, and its electromagnetic environment. This is not an issue for missions like Cassini whose magnetometer was able to provide the first signs of plumes from the south pole of Enceladus (Dougherty et al. 2006), or for the Europa Clipper whose goal is to verify the existence of a subsurface ocean, assess its conductivity, estimate its depth, and estimate the thickness of the overlying ice shell at the global scale (Howell & Pappalardo 2020). However, this space-based magnetometer approach is limited in its ability to resolve sub-global-scale lateral conductivity variations as well as the vertical conductivity profile of potentially complex stratigraphy (e.g., Kivelson et al. 1992, 1996; Styczinski & Harnett 2021). This information is best ascertained from complementary surface EM and seismic observations. Additionally, for pure magnetometer measurements, the magnetic fields generated by plasma currents surrounding the world of interest need to be characterized as they can mask the magnetic induction response of an ocean world's subsurface conductors.

In addition to orbital EM measurements, a lander-based, single-station MT or TEM measurement can provide insight into the subsurface structure. Multiple stations or nodes would increase the sensitivity to lateral conductivity variations within the ice shell. A two-station or multiple-node configuration would be especially useful around the SPT on Enceladus by bounding the conductivity and hydrological structure of the plume's plumbing structure. The TEM method has the advantage of knowing the source field parameters exactly but

would require a relatively high power source (Grimm et al. 2020).

3.3. Radar Sounding

Space-borne radars have proven to be versatile instruments in planetary exploration. They can be used as imaging radars, altimeters, or radar sounders. Side-looking radars have been used to map planetary surfaces, as in the case of Venus by the Magellan mission (Saunders & Pettengill 1991), and of Titan by the radar on board the Cassini spacecraft (Elachi et al. 2005). Magellan also performed altimetry measurements by using its nadir-looking horn antenna. Radar sounding instruments have been used successfully on the Moon and on Mars to characterize the subsurface, including the search for lava tubes and buried craters (Watters et al. 2006; Kaku et al. 2017).

Radar sounding instruments are well suited to investigate cryospheres due to the transparency of ice to radio waves for frequencies between 1 and 300 MHz (Schroeder et al. 2020). Consequently, the exploration of Mars' ice deposits, comets, and ice-covered ocean worlds can particularly benefit from the use of radar instruments. Because the radio waves penetrate deepest into the ice column for clean and cold ice, increasing temperature and impurities reduce the transparency of the ice. This resulting increase in attenuation allows clean, cold ice to be distinguished from warm, impurity-rich ice in the subsurface (Blankenship et al. 2009; Kalousová et al. 2017). Moreover, because liquid water is a strong radar reflector, subsurface water and brine reservoirs can be detected readily (Culha et al. 2020). The surface echo amplitude can be analyzed statistically to characterize the surface roughness and permittivity (i.e., snow/firn, clean/dirty ice, and brines; Grima et al. 2016), and a similar process may also be used to characterize the basal ice–water interface (Grima et al. 2019). For high-frequency (HF) radars, determination of the total electron content between the spacecraft and the surface through the dispersion of the radar signal can also be used to probe the ionosphere (Safaeinili et al. 2007; Scanlan et al. 2019).

This geophysical potential has been demonstrated by two radar sounders at Mars, the Mars Advanced Radar for Subsurface and Ionosphere Sounding (MARSIS) on the Mars Express (Jordan et al. 2009) and the Shallow Radar (SHARAD) on the Mars Reconnaissance Orbiter (MRO) (Seu et al. 2004). The heritage of SHARAD and MARSIS has led to the selection of two subsurface radar sounders on board the upcoming JUpiter ICy moon Explorer (JUICE) (Bruzzone et al. 2015) and Europa Clipper (Blankenship et al. 2018) missions. The future exploration of ocean worlds can build on this heritage enriched by new flavors of the technique, such as passive sounding that uses emissions from the host planet to sound the ice rather than an active instrument source (Schroeder et al. 2016), or bistatic radars that use large separations between receiver and transmitter antennas to, for example, infer englacial temperature distributions (Bienert et al. 2020).

3.4. Gravity and Deformation

Gravity measurements, combined with the precise determination of the surface shape, provide information about the state of the interior of the moons. Orbital gravity measurements are optimal for global-scale investigations. Tidally induced surface gravity, deformation, and tilt measurements can be more sensitive to isolated features and local effects. Depending on the required accuracy, a mission lifetime of a few months (Ermakov et al. 2021) could record the required data to meet science goals (See Table 1).

Long-wavelength characteristics are described by degree-two tidal Love numbers, h_2 quantifying the surface radial displacement, k_2 expressing the additional gravity potential induced by tides. The amplitude of long-wavelength tidal displacement is primarily controlled by the thickness and rigidity of the ice shell and only weakly depends on anelastic properties especially when the ice shell is within the conductive regime. Moreover, measuring the phase lag of h_2 and k_2 from orbit could provide constraints on dissipation within icy shells and deeper silicate interiors (Hussmann et al. 2016). Such measurements could be accomplished by multiple spacecraft or gravity rangers deployed in the equatorial region (Ermakov et al. 2021). Note, however, that signal induced by the tidal response can also be enhanced by resonant inertial waves in the subsurface oceans, which would make the tidal signal more complex (Rovira-Navarro et al. 2019).

Complementary data, including time-varying local deformation, gravity, and tilt measurements provided by a lander, would be most sensitive to the shell geometry and structure and less sensitive to the interior (silicate and metal) state. However, the time-varying surface gravity field appears to have the capacity there to reveal core signatures (Vance et al. 2021a).

On Europa, the time-varying radial displacement may reach a few to tens of meters (Moore & Schubert 2000), and static gravity anomalies could point to areas of higher heat flow suggesting local volcanism (Dombard & Sessa 2019). Titan's gravity anomalies combined with a high Love number k_2 and its rotation state point at a dense subsurface ocean with a high concentration of dissolved salts (Baland et al. 2014; Mitri et al. 2014). On Enceladus, the tidal displacement can reach up to several meters (Běhounková et al. 2017). In the SPT region, an increase in vertical deformation is coincident with the position of faults (Yin & Pappalardo 2015). Due to large variations in shell thickness and the presence of faults (Figure 3), the global and local characteristics are intertwined. This coupling results in a complex time-varying tidal deformation (Souček et al. 2019) and an apparent phase lag for h_2 and k_2. To address ice shell structure and faults, the Love number measurement, h_2, describing the surface radial displacement, needs a precision higher than 0.001 (Ermakov et al. 2021). The gravity Love number k_2 would require the same precision to distinguish between different models of the moons' interiors. Surface gravity anomalies from tides might reach several tens of μGal and be amplified by regional effects (Beuthe 2018). If a body has a dissipative and highly deformable silicate interior, the anomaly at the surface may reach 100 μGal (Figure 3).

3.5. Seismology

Seismology is capable of investigating icy ocean worlds at depths greater than just the ice shell thickness. Single-station, small-aperture arrays, and larger arrays of seismometers would likely record numerous seismic events from a wide variety of sources (see Section 1 for details on sources). A seismic array has the benefit of improved source location and observable events. However, a single-station lander, such as that on InSight's Seismic Experiment for Interior Structure (SEIS; Banerdt et al. 2020; Giardini et al. 2020), can also detect and locate sources.

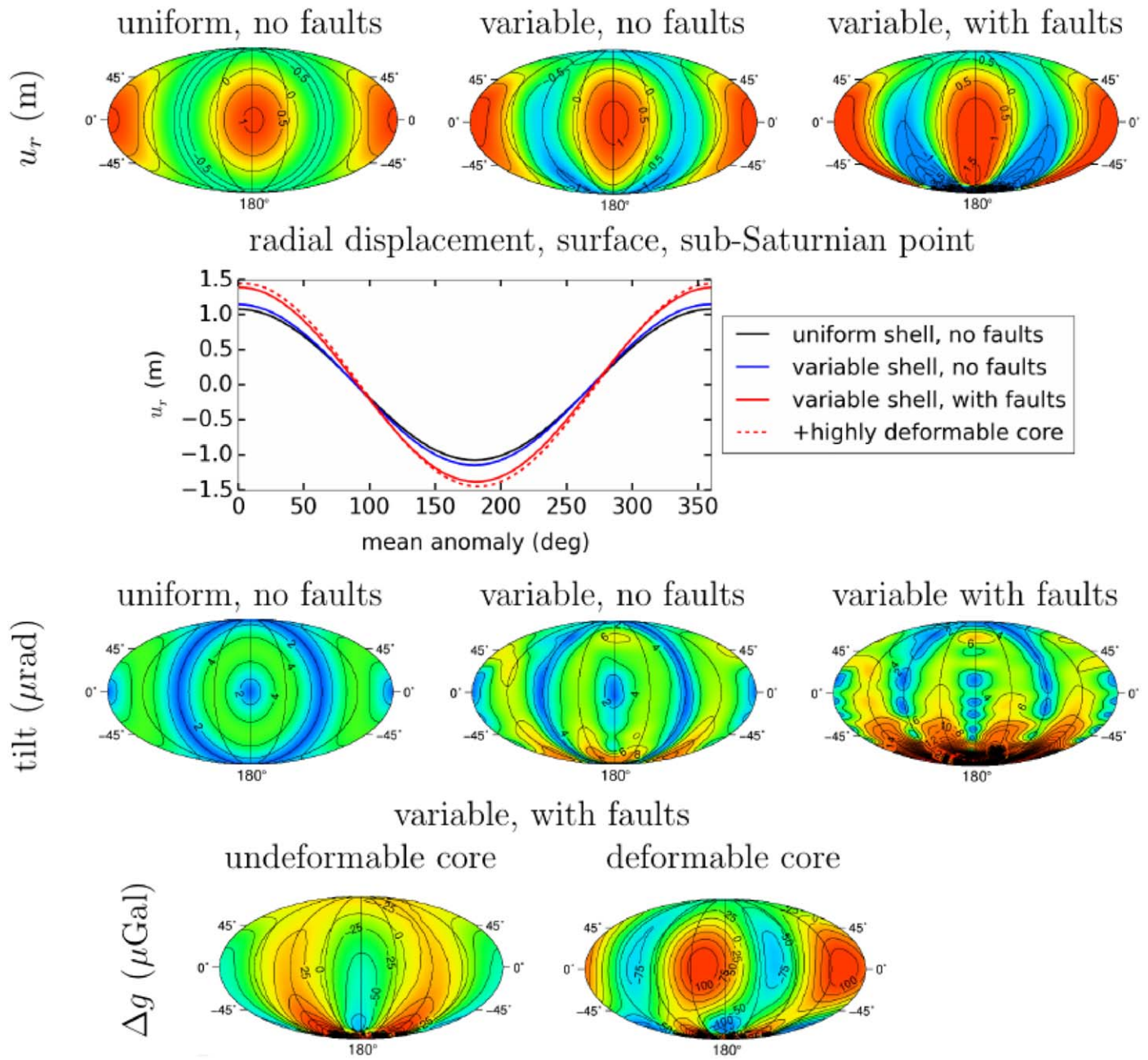

Figure 3. Surface displacement, tilt, and gravity field for Enceladus. Surface radial displacement (*ur*) and tilt are for models with uniform or variable ice shell thickness (average thickness 20 km) and with or without faults. Gravity anomalies (Δg) at the surface are for the model with and without a deformable core (i.e., the silicate interior) and aand variable ice shell thickness with faults. Results based on an elastic ice shell and highly deformable and dissipative (>50 GW) parameterized silicate interior. All maps are shown at periapsis. Models are based on the Souček et al. (2019) model.

The sources themselves, along with the waveforms they produce, provide a wealth of information regarding the activity of the ice shells and deeper interior structure. Estimates of seismic noise (Panning et al. 2018, 2020a) suggest that even geophones would be able to record some larger or local seismic events, while more sensitive broadband instruments, such as an STS2, would be able to record more events from greater distances and should be able to record the peak of background noise energy (Figure 4). Several tidal cycles worth of data would likely be required in order to determine the seismicity, as well as to identify and locate events to use for internal structure recovery.

The locations and source parameters of detected seismic events can provide context for dynamics within the ice shells. Data from seismometers would be tested for correlations with tidal cycle or temperature measurements to investigate how the ice shell is influenced by its environment (Lombardi et al. 2019; Marusiak et al. 2019; Olinger et al. 2019). The depths of detected events would hint at the transition between ductile and brittle ice. Seismic sources might also reveal the presence of local heterogeneities within the ice shells, such as liquid pockets or cryomagma chambers. These pockets are analogous to aquifers and subglacial lakes (Peters et al. 2008) on Earth and would be detectable through similar approaches. Reflections off ice–water interfaces and seismic inversions would

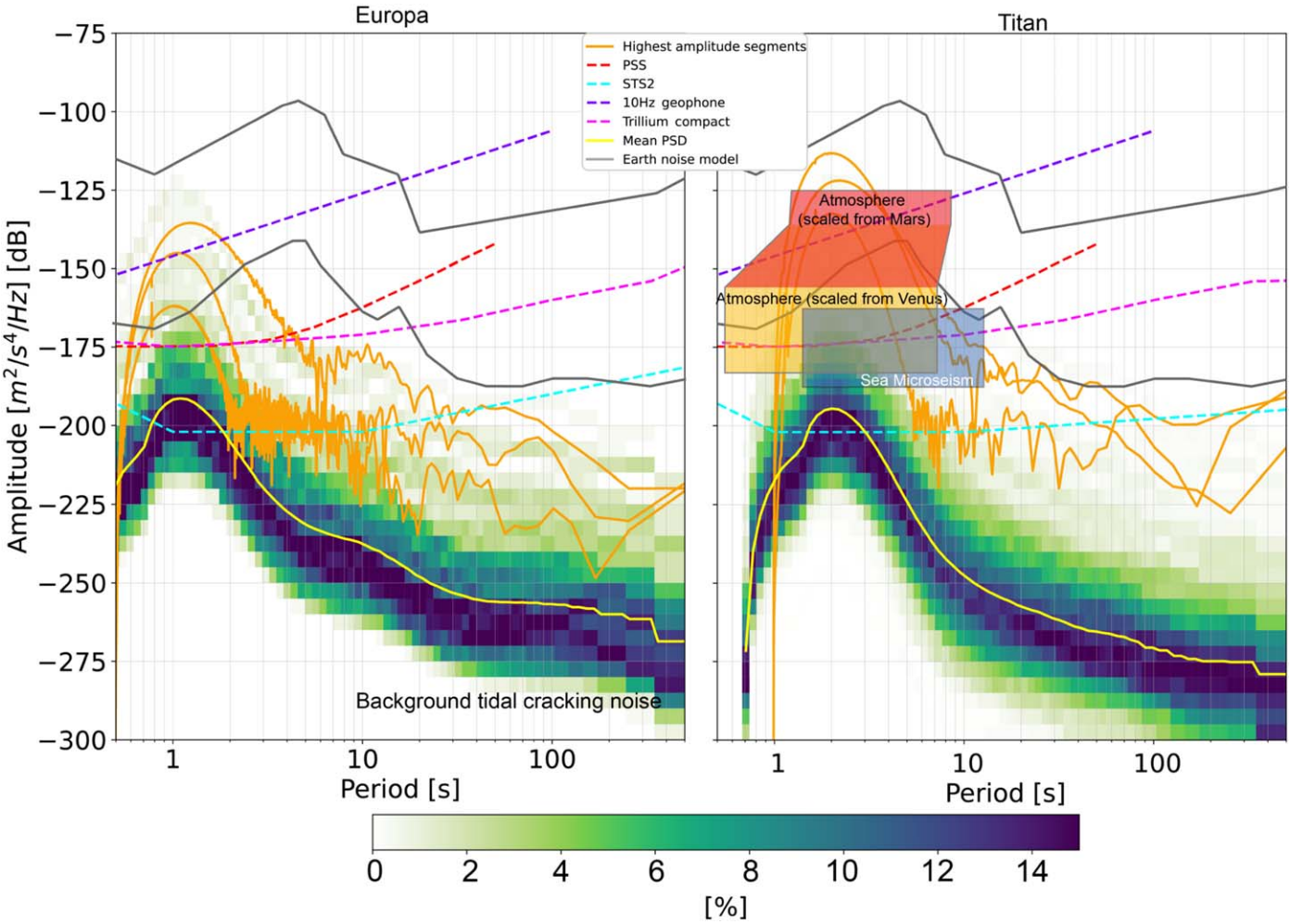

Figure 4. Probability power spectral densities (PPSDs) for Europa (left) and Titan (right). The color bar indicates the probability of a signal having a given amplitude at a given period. Noise levels of several seismic instruments are plotted along with the Earth noise levels for reference. Seismic noise models are based on Panning et al. (2018) for Europa and Panning et al. (2020a) for Titan.

reveal the depth of such pockets and constrain the thickness of the water layers. On Titan, it is possible to also have pockets of liquid methane entrained in the surface ice shell (Hayes et al. 2008).

To estimate ice shell thickness, a seismometer can use trapped Crary waves (Ewing et al. 1934; Panning et al. 2018). The resonant frequencies of these waves (f_{Cr}) are dependent on the ice shell thickness, according to the following relationship (Crary 1954; Stähler et al. 2018):

$$f_{\mathrm{Cr}} = \frac{(n+1)v_S}{2d\sqrt{1-\left(\frac{v_S}{v_P}\right)^2}}, \quad (1)$$

where n is a non-negative integer, v_S and v_P are the S and P velocities, and d is the ice shell thickness. For Europa and Enceladus, which likely have ice shells thinner than 40 km, the fundamental Crary wave resonance ($n = 0$) is above 0.1 Hz, measurable by space-ready seismometers (Lognonné et al. 2019; Marusiak et al. 2021). The average ice shell thickness can also be determined with a frequency–time analysis (FTAN) of the surface wave energy recorded in the vertical plane connecting the source and receiver. If the wavelength of the surface wave is less than the thickness of the ice shell, the wave will behave like a classical Rayleigh wave. For wavelengths greater than the thickness of the ice shell, however, the seismic waves will behave like flexural waves, with dispersions that are independent of the seismic velocity gradient, which have a characteristic group velocity maximum that depends on the ice shell thickness (e.g., Panning et al. 2006). For Titan, with a thicker ice shell, body waves reflecting off the ice–ocean interface can be used to place estimates on the ice shell thickness and seismic velocity. However, due to the curvature of that moon and the likelihood of a variably thick ice shell, these waves may only be detectable for sources within 50° epicentral distance.

3.6. Subsurface Camera: Real-time, In Situ Geophysical Imaging within Sensor Networks

A landed geophysical sensor network can be created to sense and process geophysical waveform signals and compute a subsurface image in situ and in real time. In situ computing and imaging allows real-time continuous monitoring and significant data reduction, avoiding costly manual data collection or massive raw data telemetry over the wireless or satellite links. Just like an optical camera generates photos and videos from received light waves, such a system can be said of a subsurface

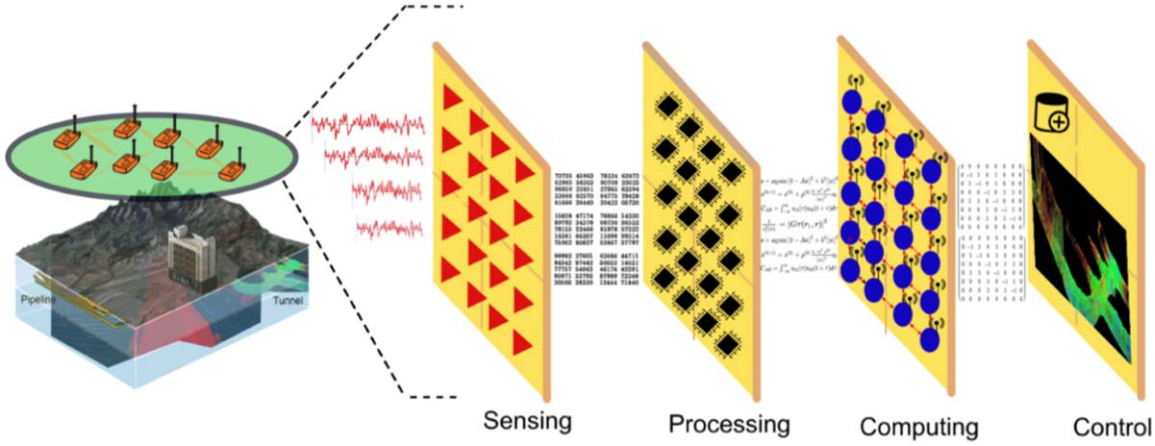

Figure 5. Schematic of a subsurface camera enabling real-time geophysical imaging within sensor networks. Figure from Song et al. (2019).

camera (Song et al. 2019) that generates subsurface images and videos from received geophysical waves. The basic mechanism (Figure 5) of a subsurface camera is as follows: geophysical waves propagating/reflected/refracted through the subsurface enter a geophysical sensor network, where the subsurface image will be computed (based on inversion and other methods) and recorded; a control software with graphical user interface (GUI) can be connected to this network to visualize computed images and adjust settings such as resolution, filter, regularization, and other algorithm parameters. In seismic sensor networks, the travel-time tomography (Shi et al. 2013), ambient noise tomography (Valero et al. 2018; Wang et al. 2020), and microseismic imaging (Sun et al. 2015) have been designed and demonstrated. Four layers are envisioned in the architecture of a subsurface camera: sensing, processing, computing, and control. A subsurface camera system may incorporate one or more types of geophysical sensors and imaging algorithms based on application needs. Various geophysical sensors and methods have been used for subsurface explorations: seismic methods, electrical methods, geodesy and gravity techniques, magnetic techniques, electrical conductivity tomography, electromagnetic methods, etc. Different geophysical sensors/methods are sensitive to different geophysical subsurface properties. Different geophysical waves (Erkan 2008) have different wavelengths and can probe the subsurface at different ranges and resolutions. Waves with a longer wavelength typically propagate deeper and farther but generate lower-resolution images. For example, in seismology, the vertical resolution is typically $\approx 1/4$ of the wavelength (Kearey et al. 2002). Through earthquake seismology, the entire Earth can be imaged but at a much lower resolution than when using reflection or refraction seismology, which can only image the top 10 and 150 km, respectively. Integrating different geophysical methods and in situ computing to generate comprehensive subsurface images will be a transformative research direction with the potential to be a major advance in planetary exploration.

3.7. Analog Studies and Laboratory Measurements

Prior to mission data collection, analog and laboratory studies can be critical for mission success. As with Earth, the power of geophysical probing techniques relies on our knowledge of the physical properties of materials at the relevant conditions (e.g., density, sound speed, thermal properties, conductivity, etc.). Pressure, temperature, and composition conditions in icy oceans worlds vary widely and mostly lie in ranges largely unexplored experimentally for the relevant materials (e.g., ices, liquids, and hydrates). This lack of experimental data may inhibit the development of advanced and realistic methods for forward and inverse geophysical modeling.

Key material properties include density for gravity measurements, electrical conductivity for geomagnetic measurements, relative permittivity for radar, and velocities (related to elastic properties) for seismology. The large temperature gradient within the first few kilometers of the ice shell, from $\approx$100 K at the surface to $\approx$260 K in the convective ice, may result in a large variation in these properties. For example, the temperature and pressure dependencies of seismic velocities of ice Ih have been measured down to 253 K and 100 MPa (Helgerud et al. 2009) and showed a large temperature dependency. At colder conditions, like those found at the surface, no experimental measurement currently exists. Only recent predictions from thermodynamic and statistical physics models have studied the effect at near-surface conditions (Journaux et al. 2020a). Journaux et al. (2020a, 2020b) showed the compressive wave velocity, V_P, within the ice shell decreases from $\approx 4200\,\mathrm{m\,s^{-1}}$ at 100 K and no (0) pressure to $\approx 3900\,\mathrm{m\,s^{-1}}$ at 260 K and 50 MPa. Most of the seismic speed variation is concentrated in the first few kilometers within the conductive ice shell (Figure 6). Below, in the convective portion of the ice shell, the temperature is near constant, resulting in near-constant velocity. The decreasing velocity with depth near the surface is typically not observed in the near-surface Earth. The negative velocity gradient will alter the distances at which body waves can be observed and will alter the appearance of surface waves. Further experimental studies on seismic velocities at colder conditions are necessary as current conclusions rely on theoretical predictions, which ignore the effects of anisotropy, porosity, or presence of other crystalline solids (e.g., gas clathrates, salt hydrates, etc.).

In addition to laboratory experiments, field work can provide key insights for mission implementation. For example, terrestrial geophysical analog studies of icy ocean worlds have illustrated the utility of a single-station seismometer and small-aperture array (Marusiak 2020) compared to larger, more traditional seismic deployments. While time-consuming and relatively massive deployment systems to put seismometers on the ground can be important for maximizing sensitivity

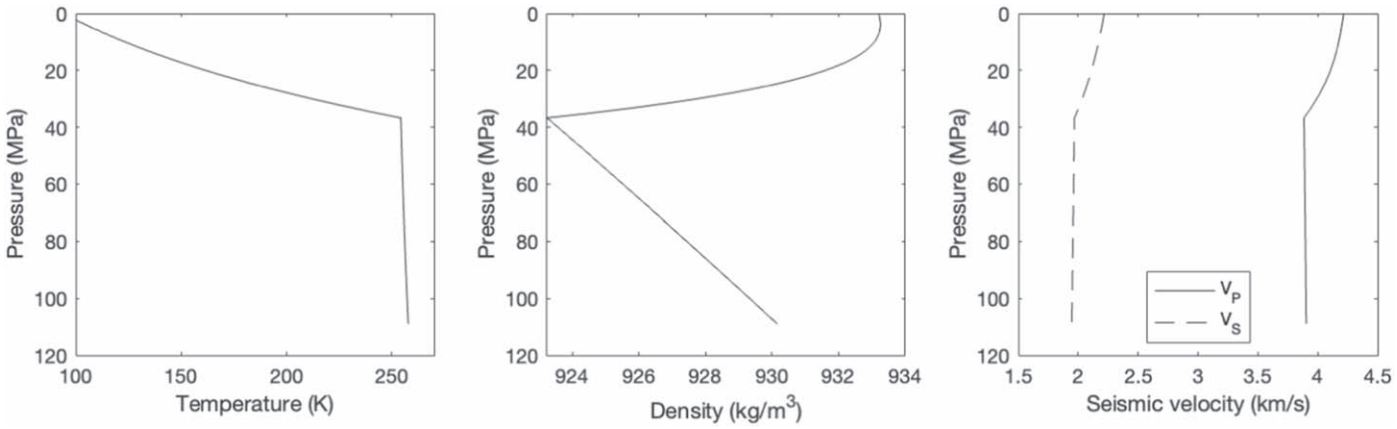

Figure 6. Physical property profiles of an ≈85 km pure ice Ih shell for Titan computed using PlanetProfile (Vance et al. 2018) for the thermal profile and SeaFreeze (Journaux et al. 2020a) for the thermodynamic properties. The conductive ice thickness is ≈30 km in this example.

(Banerdt et al. 2020; Panning et al. 2020b), seismometers in a lander vault or on deck may be necessary to make ocean world missions possible (e.g., Hand et al. 2017). In this case, both analog field deployments in icy settings (Marusiak et al. 2021) and in controlled experiments with a spacecraft engineering model (Panning & Kedar 2019) show an on-deck deployment can record similar seismic responses across a wide range of frequencies, compared to a ground-coupled instrument when wind and thermal effects are properly mitigated. However, poor coupling of instruments to the deck and exposure to an atmosphere would greatly increase the background noise (Marusiak et al. 2020b). For Enceladus and Europa, wind effects are expected to be minimal due to lack of an atmosphere but will be a significant source of noise for Titan.

Radar sounding investigations of ice shelves in Antarctica and the Arctic have similarly validated the use of ice-penetrating radar for ocean worlds (e.g., Blankenship et al. 2009). Moreover, novel analysis techniques developed for the terrestrial cryosphere can also be applicable to icy satellites, such as relating the characteristics of basal reflectors to melting and freezing processes operating beneath the ice—which are in turn related to oceanographic conditions (e.g., Jenkins et al. 2006; Nicholls et al. 2015). Laboratory investigations could additionally provide valuable insights regarding remote signatures of ice shell processes, such as the dielectric properties of natural ices that are poorly constrained (e.g., MacGregor et al. 2007) and essential for the success of planned and future missions exploring the ice shells of ocean worlds using radar sounding and electromagnetics.

4. Conclusions

The geophysical investigations described above would enhance our knowledge of the current state, structure, and potential habitability of icy ocean worlds. Orbiters, similar to the Europa Clipper mission (Phillips & Pappalardo 2014), landers such as the proposed Europa lander (Hand et al. 2017), or missions comprising both a lander and an orbiter (Mackenzie et al. 2021) should be considered for future missions. While a single lander would be able to accomplish numerous goals, a networked implementation would provide a leap in capability to understand icy satellites, including the processes and properties supporting habitability. Continued innovation in planetary geophysics requires additional research and analysis, modeling and technical implementation, development of autonomous networked stations, and investments in new sensors and electronics. Laboratory and analog field work should also be continued to evaluate new instrumentation and approaches.

A portion of this research was carried out at the Jet Propulsion Laboratory, California Institute of Technology, under a contract with the National Aeronautics and Space Administration (Habitable Worlds Grant: 16-HW16_2-0065) and JPL's Strategic Research and Technology Development program. We thank Natalie Wolfenbarger and Edwin Kite for helpful discussions, as well as the suggestions of two anonymous reviewers.

ORCID iDs

Angela G Marusiak https://orcid.org/0000-0001-6925-1383
Steven Vance https://orcid.org/0000-0002-4242-3293
Mark P Panning https://orcid.org/0000-0002-2041-3190
Marie Běhounková https://orcid.org/0000-0001-8227-0685
Paul K Byrne https://orcid.org/0000-0002-5644-7069
Gaël Choblet https://orcid.org/0000-0002-0220-9233
Mohit Melwani Daswani https://orcid.org/0000-0002-4611-3209
Kynan Hughson https://orcid.org/0000-0002-5714-3526
Baptiste Journaux https://orcid.org/0000-0002-0957-3177
Ana H Lobo https://orcid.org/0000-0003-3862-1817
Britney E Schmidt https://orcid.org/0000-0001-7376-8510
Kateřina Pleiner Sládková https://orcid.org/0000-0001-6486-1692
Krista M Soderlund https://orcid.org/0000-0002-7901-3239
WenZhan Song https://orcid.org/0000-0001-8174-1772
Ondřej Souček https://orcid.org/0000-0002-6515-5420
Gregor Steinbrügge https://orcid.org/0000-0002-1050-7759
Andrew F. Thompson https://orcid.org/0000-0003-0322-4811
Sili Wang https://orcid.org/0000-0002-3672-1243

References

Amit, H., Choblet, G., Tobie, G., et al. 2020, Icar, 338, 113509
Baland, R. M., Tobie, G., Lefèvre, A., & Van Hoolst, T. 2014, Icar, 237, 29
Banerdt, W. B., Smrekar, S. E., Lognonné, P., et al. 2020, NatGe, 13, 183
Barge, L. M., & White, L. M. 2017, AsBio, 17, 820
Beuthe, M. 2018, Icar, 302, 145
Beuthe, M., Rivoldini, A., & Trinh, A. 2016, GeoRL, 43, 10088

Bienert, N. L., Schroeder, D. M., Peters, S. T., et al. 2020, AGUFM, 2020, NS003-0002
Bland, M. T., & McKinnon, W. B. 2017, AAS/DPS Meeting, 49, 203.02
Blankenship, D., Ray, T., Plaut, J., et al. 2018, in 42nd COSPAR Scientific Assembly 42, B5.3-55-18
Blankenship, D. D., Young, D. A., Moore, W. B., & Moore, J. C. 2009, Europa (Tucson, AZ: Univ. Arizona Press), 631
Bruzzone, L., Plaut, J. J., Alberti, G., et al. 2015, in 2015 IEEE Int. Geoscience and Remote Sensing Symp. (IGARSS) (Piscataway, NJ: IEEE), 1257
Buffo, J. J., Schmidt, B. E., Huber, C., & Walker, C. C. 2020, JGRE, 125, e06394
Běhounková, M., Souček, O., Hron, J., & Čadek, O. 2017, AsBio, 17, 941
Běhounková, M., Tobie, G., Choblet, G., et al. 2021, GeoRL, 48, e90077
Čadek, O., Kalousová, K., Kvorka, J., & Sotin, C. 2021, Icar, 364, 114466
Čadek, O., Souček, O., Běhounková, M., et al. 2019, Icar, 319, 476
Čadek, O., Tobie, G., Van Hoolst, T., et al. 2016, GeoRL, 43, 5653
Carr, M. H., Belton, M. J. S., Chapman, C. R., et al. 1998, Natur, 391, 363
Casajus, L. G., Zannoni, M., Modenini, D., et al. 2021, Icar, 358, 114187
Choblet, G., Tobie, G., Sotin, C., et al. 2017, NatAs, 1, 841
Crary, A. P. 1954, TrAGU, 35, 293
Creighton, A. L., Parsekian, A. D., Angelopoulos, M., et al. 2018, JGRB, 123, 9310
Culha, C., Schroeder, D. M., Jordan, T. M., & Haynes, M. S. 2020, Icar, 339, 113578
Dombard, A. J., & Sessa, A. M. 2019, Icar, 325, 31
Dougherty, M. K., Khurana, K. K., Neubauer, F. M., et al. 2006, Sci, 311, 1406
Dybing, S. N., Ringler, A. T., Wilson, D. C., & Anthony, R. E. 2019, BuSSA, 109, 1082
Elachi, C., Wall, S., Allison, M., et al. 2005, Sci, 308, 970
Erkan, K. 2008, PhD thesis, Ohio State Univ. Columbus https://core.ac.uk/download/pdf/159585702.pdf
Ermakov, A., Park, R., Roa, J., et al. 2021, PSJ, in press
Ewing, M., Crary, A. P., & Thorne, A. M. J. 1934, Physi, 5, 181
Fagents, S. A., Greeley, R., Sullivan, R. J., et al. 2000, Icar, 144, 54
Giardini, D., Lognonné, P., Banerdt, W. B., et al. 2020, NatGe, 13, 205
Gissinger, C., & Petitdemange, L. 2019, NatAs, 3, 401
Glein, C. R., & Waite, J. H. 2020, GeoRL, 47, e85885
Greeley, R., Figueredo, P. H., Williams, D. A., et al. 2000, JGRE, 105, 22559
Greeley, R., Sullivan, R., Klemaszewski, J., et al. 1998, Icar, 135, 4
Greenberg, R., Geissler, P., Hoppa, G. V., et al. 1998, Icar, 135, 64
Greenberg, R., Hoppa, G. V., Bart, G., & Hurford, T. A. 2003, CeMDA, 87, 171
Grima, C., Greenbaum, J. S., Lopez Garcia, E. J., et al. 2016, GeoRL, 43, 7011
Grima, C., Koch, I., Greenbaum, J., et al. 2019, JGlac, 65, 675
Grimm, R., Delory, G., Espley, J., & Stillman, D. 2020, LPSC, 51, 1568
Grimm, R. E. 2002, JGRE, 107, 5006
Grimm, R. E. 2003, JGRE, 108, 8037
Gutenberg, B. 1947, Journal of Meteorology, 4, 21
Halevy, I., & Bachan, A. 2017, Sci, 355, 1069
Hand, K. P., Murray, A. E., Garvin, J. B., et al. 2017, Report of the Europa Science Definition Team, Tech. Rep., https://europa.nasa.gov/resources/58/europa-lander-study-2016-report/
Hayes, A., Aharonson, O., Callahan, P., et al. 2008, GeoRL, 35, L09204
Hayes, A., Lorenz, R., Donelan, M., et al. 2013, Icar, 225, 403
Helgerud, M. B., Waite, W. F., Kirby, S., & Nur, A. 2009, JGRB, 114, B02212
Helgerud, M. B., Waite, W. F., Kirby, S. H., & Nur, A. 2003, CaJPh, 81, 47
Hemingway, D. J., & Mittal, T. 2019, Icar, 332, 111
Hoppa, G. V. 1999, Sci, 285, 1899
Howell, S. 2020, in Europlanet Science Congress 2020 (Göttingen: Copernicus GmbH), EPSC2020-173, doi:10.5194/epsc2020-173
Howell, S. M., & Pappalardo, R. T. 2019, Icar, 322, 69
Howell, S. M., & Pappalardo, R. T. 2020, NatCo, 11, 1311
Hurford, T. A., & Greenberg, R. 2005, PhD thesis, Univ. Arizona
Hurford, T. A., Henning, W., Maguire, R., et al. 2020, Icar, 338, 113466
Hurford, T. A., Sarid, A. R., & Greenberg, R. 2007, Icar, 186, 218
Hussmann, H., Shoji, D., Steinbrügge, G., Stark, A., & Sohl, F. 2016, CeMDA, 126, 131
Iess, L., Stevenson, D. J., Parisi, M., et al. 2014, Sci, 344, 78
Jansen, M. F. 2016, JPO, 46, 1917
Jenkins, A., Corr, H. F., Nicholls, K. W., Stewart, C. L., & Doake, C. S. 2006, JGlac, 52, 325
Johnson, B. C., Sheppard, R. Y., Pascuzzo, A. C., Fisher, E. A., & Wiggins, S. E. 2017, JGRE, 122, 2765
Jordan, R., Picardi, G., Plaut, J., et al. 2009, P&SS, 57, 1975
Journaux, B., Brown, J. M., Pakhomova, A., et al. 2020a, JGRE, 125, e06176
Journaux, B., Kalousová, K., Sotin, C., et al. 2020b, SSRv, 216, 7
Kaku, T., Haruyama, J., Miyake, W., et al. 2017, GeoRL, 44, 10,155
Kalousová, K., Schroeder, D. M., & Soderlund, K. M. 2017, JGRE, 122, 524
Kalousová, K., & Sotin, C. 2020, GeoRL, 47, e2020GL087481
Kamata, S., Nimmo, F., Sekine, Y., et al. 2019, NatGe, 12, 407
Kang, W., Mittal, T., Bire, S., Campin, J.-M., & Marshall, J. 2021, arXiv:2104.07008
Kargel, J. S., & Pozio, S. 1996, Icar, 119, 385
Katterhorn, S. A., & Hurford, T. A. 2009, in Europa, ed. R. Pappalardo, W. B. McKinnon, & K. Khurana (Tucson, AZ: Univ. Arizona Press), 199
Kattenhorn, S. A., & Prockter, L. M. 2014, NatGe, 7, 762
Kearey, P., Brooks, M., & Hill, I. 2002, An Introduction to Geophysical Exploration (3rd ed.; Oxford: Blackwell)
Kimura, J., Hussmann, H., Kamata, S., et al. 2019, JSAST, 17, 234
Kirchoff, M. R., & Schenk, P. 2009, Icar, 202, 656
Kite, E. S., & Rubin, A. M. 2016, PNAS, 113, 3972
Kivelson, M., Khurana, K., Russell, C., et al. 2000, Sci, 289, 1340
Kivelson, M. G., Khurana, K. K., Means, J. D., Russell, C. T., & Snare, R. C. 1992, SSRv, 60, 357
Kivelson, M. G., Khurana, K. K., Russell, C. T., et al. 1996, Natur, 384, 537
Kvorka, J., Čadek, O., Tobie, G., & Choblet, G. 2018, Icar, 310, 149
Lobo, A., Thompson, A., Vance, S., & Tharimena, S. 2021, NatGe, 14, 185
Lognonné, P., Banerdt, W. B., Giardini, D., et al. 2019, SSRv, 215, 12
Lombardi, D., Gorodetskaya, I., Barruol, G., & Camelbeeck, T. 2019, AnGla, 60, 45
Lorenz, R. D., Newman, C. E., Tokano, T., et al. 2012, P&SS, 70, 73
Lucchetti, A., Pozzobon, R., Mazzarini, F., Cremonese, G., & Massironi, M. 2017, Icar, 297, 252
Lunine, J. I. 2010, FaDi, 147, 405
Lunine, J. I., & Stevenson, D. J. 1985, ApJS, 58, 493
MacGregor, J. A., Winebrenner, D. P., Conway, H., et al. 2007, JGRF, 112, F03008
Mackenzie, S. M., Neveu, M., Davila, A. F., et al. 2021, PSJ, 2, 77
Marusiak, A. G. 2020, PhD thesis, Univ. Maryland doi:10.13016/jrd0-dofk
Marusiak, A. G., Panning, M. P., & Vance, S. D. 2020a, AGUFM, P086-01
Marusiak, A. G., Schmerr, N. C., Avenson, B., et al. 2019, AGUFM, doi:10.1002/essoar.10501282.1
Marusiak, A. G., Schmerr, N. C., Avenson, B., et al. 2021, Seismological Research Letters, 92, 2036
Marusiak, A. G., Schmerr, N. C., DellaGiustina, D. N., et al. 2020b, Seismological Research Letters, 91, 1901
Matsuyama, I., Beuthe, M., Hay, H. C., Nimmo, F., & Kamata, S. 2018, Icar, 312, 208
McEwen, A. 1986, Natur, 321, 49
McKinnon, W. B. 2015, GeoRL, 42, 2137
Mitri, G., Meriggiola, R., Hayes, A., et al. 2014, Icar, 236, 169
Moore, W. B., & Hussmann, H. 2009, in Europa, ed. R. T. Pappalardo, W. B. McKinnon, & K. K. Khurana (Tucson, AZ: Univ. Arizona Press), 369
Moore, W. B., & Schubert, G. 2000, Icar, 147, 317
Mousis, O., Chassefière, E., Holm, N. G., et al. 2015, AsBio, 15, 308
Neveu, M., Hays, L. E., Voytek, M. A., New, M. H., & Schulte, M. D. 2016, AsBio, 18, 1375
Nicholls, K. W., Corr, H. F., Stewart, C. L., et al. 2015, JGlac, 61, 1079
Nimmo, F., Giese, B., & Pappalardo, R. T. 2003, GeoRL, 30, 1233
Nimmo, F., & Schenk, P. 2006, JSG, 28, 2194
Noll, K. S., Weaver, H. A., & Gonnella, A. M. 1995, JGRE, 100, 19057
Olinger, S. D., Lipovsky, B. P., Wiens, D. A., et al. 2019, GeoRL, 46, 6644
Panning, M., Lekic, V., Manga, M., Cammarano, F., & Romanowicz, B. 2006, JGRE, 111, E12008
Panning, M. P., & Kedar, S. 2019, Icar, 317, 373
Panning, M. P., Lorenz, R., Shiraishi, H., et al. 2020a, SEG Technical Program Expanded Abstracts 2020 (Tulsa, OK: Society of Exploration Geophysicists), 3539, doi:10.1190/segam2020-3426937.1
Panning, M. P., Pike, W. T., Lognonné, P., et al. 2020b, JGRE, 125, e06353
Panning, M. P., Stähler, S. C., Vance, S. D., et al. 2018, JGRE, 123, 163
Paranicas, C., Mauk, B. H., Khurana, K., et al. 2007, GeoRL, 34, L15103
Peters, L. E., Anandakrishnan, S., Holland, C. W., et al. 2008, GeoRL, 35, L23501
Phillips, C. B., & Pappalardo, R. T. 2014, EOSTr, 95, 165
Porco, C. C., Helfenstein, P., Thomas, P. C., et al. 2006, Sci, 311, 1393
Postberg, F., Schmidt, J., Hillier, J., Kempf, S., & Srama, R. 2011, Natur, 474, 620
Rhoden, A. R., Hurford, T. A., Spitale, J., et al. 2020, E&PSL, 544, 116389
Rignot, E., Mouginot, J., & Scheuchl, B. 2011, Sci, 333, 1427, LP
Roberts, J. H. 2015, Icar, 258, 54
Rovira-Navarro, M., Rieutord, M., Gerkema, T., et al. 2019, Icar, 321, 126
Russell, M. J., Barge, L. M., Bhartia, R., et al. 2014, AsBio, 14, 308

Russell, M. J., Murray, A. E., & Hand, K. P. 2017, AsBio, 17, 1265
Safaeinili, A., Kofman, W., Mouginot, J., et al. 2007, GeoRL, 34, L23204
Sandwell, D., Rosen, P., Moore, W., & Gurrola, E. 2004, JGRE, 109, E11003
Saunders, R. S., & Pettengill, G. H. 1991, Sci, 252, 247
Scanlan, K. M., Grima, C., Steinbrügge, G., et al. 2019, P&SS, 178, 104696
Schenk, P. M., & Zahnle, K. 2007, Icar, 192, 135
Schmidt, B. E., Blankenship, D. D., Patterson, G. W., & Schenk, P. M. 2011, Natur, 479, 502
Schroeder, D. M., Bingham, R. G., Blankenship, D. D., et al. 2020, AnGla, 61, 1
Schroeder, D. M., Romero-Wolf, A., Carrer, L., et al. 2016, P&SS, 134, 52
Schulze-Makuch, D., & Irwin, L. 2002, AsBio, 2, 105
Seu, R., Biccari, D., Orosei, R., et al. 2004, P&SS, 52, 157
Shi, L., Song, W., Xu, M., et al. 2013, in IEEE Int. Conf. on Distributed Computing in Sensor Systems (Piscataway, NJ: IEEE), 1
Soderlund, K. M. 2019, GeoRL, 46, 8700
Soderlund, K. M., Kalousová, K., Buffo, J. J., et al. 2020, SSRv, 216, 1
Soderlund, K. M., Schmidt, B. E., Wicht, J., & Blankenship, D. D. 2014, NatGe, 7, 16
Song, W., Li, F., Valero, M., & Zhao, L. 2019, Senso, 19, 301
Sotin, C., Tobie, G., Wahr, J., & McKinnon, W. B. 2009, in Europa, ed. R. Pappalardo, W. B. McKinnon, & K. Khurana (Tucson, AZ: Univ. Arizona Press), 85
Souček, O., Běhounková, M., Čadek, O., et al. 2019, Icar, 328, 218
Sparks, W. B., Hand, K. P., McGrath, M. A., et al. 2016, ApJ, 829, 121
Stähler, S. C., Panning, M. P., Hadziioannou, C., et al. 2019, E&PSL, 520, 250
Stähler, S. C., Panning, M. P., Vance, S. D., et al. 2018, JGRE, 123, 206
Steinbrügge, G., Stark, A., Hussmann, H., Sohl, F., & Oberst, J. 2015, P&SS, 117, 184
Steinbrügge, G., Steinke, T., Thor, R., Stark, A., & Hussmann, H. 2019, Geosc, 9, 320
Steinbrügge, G., Voigt, J. R. C., Wolfenbarger, N. S., et al. 2020, GeoRL, 47, e90797
Styczinski, M. J., & Harnett, E. M. 2021, Icar, 354, 114020
Sun, J., Zhu, T., Fomel, S., et al. 2015, in SEG Annual Meeting 2015 (Richardson, TX: Society of Exploration Geophysicists), 2485
Travis, B. J., Palguta, J., & Schubert, G. 2012, Icar, 218, 1006
Turtle, E. P., & Pierazzo, E. 2001, Sci, 294, 1326
Valero, M., Li, F., Wang, S., Lin, F.-C., & Song, W. 2018, in IEEE Transactions on Signal and Information Processing over Networks (Piscataway, NJ: IEEE), 375
Vance, S., Behounkova, M., Bills, B., et al. 2021a, White Paper to the Decadal Survey, https://assets.pubpub.org/qd8r6tyb/31617915309014.pdf
Vance, S., & Goodman, J. 2009, Europa (Tucson, AZ: Univ. Arizona Press), 459
Vance, S. D., Journaux, B., Hesse, M., & Steinbrügge, G. 2021b, JGRE, 126, e06736
Vance, S. D., Panning, M. P., Stähler, S., et al. 2018, JGRE, 123, 180
Vance, S. D., Styczinski, M. J., Bills, B. G., et al. 2021c, JGRE, 126, e06418
Wahr, J. M., Zuber, M. T., Smith, D. E., & Lunine, J. I. 2006, JGRE, 111, E12005
Waite, J. H., Glein, C. R., Perryman, R. S., et al. 2017, Sci, 356, 155
Wang, S., Li, F., Panning, M., et al. 2020, in IEEE Transactions on Signal and Information Processing over Networks (Piscataway, NJ: IEEE), 656
Watters, T. R., Leuschen, C. J., Plaut, J. J., et al. 2006, Natur, 444, 905
Yin, A., & Pappalardo, R. T. 2015, Icar, 260, 409
Zahnle, K., Schenk, P., Levison, H., & Dones, L. 2003, Icar, 163, 263
Zhu, P., Manucharyan, G. E., Thompson, A. F., Goodman, J. C., & Vance, S. D. 2017, GeoRL, 44, 5969
Zonge, K. L., & Hughes, L. J. 1991, Electromagnetic Methods in Applied Geophysics: Vol. 2, Application, Parts A and B (Tulsa, OK: Society of Exploration Geophysicists), 713, doi:10.1190/1.9781560802686.ch9